Supporting Information

Ag nanowire synthesis

All the chemicals were purchased from Sigma Aldrich and used without further purification. The synthesis of Ag nanowires was performed according to the polyol process [1], with ethylene glycol (EG) acting both as the solvent and the reducing agent. Briefly, 5 mL of anhydrous EG were heated up to 154 ºC in an oil bath for 1h, before adding 400 µL of $CuCl_2$ (4mM in EG). After 15 min, 3 mL of polyvinylpyrrolidone (0.147 M in EG) were added to the solution within 10 s. Then 3 mL of $AgNO_3$ (0.094 M in EG) were added drop-wise within 10 min. The $AgNO_3$ solution was sonicated for 6 min prior to the injection. N_2 was bubbled through the entire process, and the vial was sealed to prevent oxygen from entering. The reaction was stopped after ~ 90 min and the nanowires were collected by centrifugation (3000 RPM) and cleaned several times in acetone and water and redispersed in 2 mL of deionized water. The average diameter of the nanowires was estimated to be in the 60-90 nm range and the length between 10 and 20 µm. A small amount of nanoparticle byproduct was observed.

Quasi-monocrystalline Cu₂O shell growth

All the chemicals were purchased from Sigma Aldrich and used without further purification. The growth of a cuprous oxide shell around the Ag nanowires was conducted following a reported procedure for the synthesis of metal-Cu_2O core-shell nanoparticles, with some modifications [2]. 100 µL of $CuCl_2$ (0.1 M in water) were added to 9.8 mg of deionized water at room temperature, followed by the addition of 87 mg of sodium dodecyl sulfate (SDS). After SDS dissolution, 50 µL of the previously synthesized Ag nanowires were injected in the solution. Note that the shell thickness can be controlled by the amount of Ag nanowires added to the solution. 250 µL of NaOH (1M in water) were added, followed by 150 µL of NH_2OH HCl (0.2 M in water). After 2 hours the core-shell nanowires were cleaned several times in water and ethanol by centrifugation (3000 RPM) and then redispersed in ethanol.

Focused Ion Beam (FIB) cross-section

The cross-section shown in Fig. 2c is realized by exposing the core-shell nanowire to a focused beam of gallium ions, that upon impact mills the sample in a precise and controlled manner. A 500 nm layer of platinum was deposited in-situ prior to the ion beam exposure for obtaining a sharper cut. The ablation reveals the details underneath the surface of the core-shell nanowire, which is hence imaged with secondary electrons (SE), confirming the presence of a core-shell nanostructure. The HELIOS^TM NANOLAB 660 (FEI) microscope was employed for the process.

Structural/Chemical characterization

The TITAN^TM microscope 80-300kV (FEI) was used for TEM measurements and electron diffraction. The VERIOS^TM 460L XHR (FEI) was employed for SEM imaging. Bruker D2 was used for XRD measurements.

Optical characterization

After synthesis the core-shell nanowires were drop-cast from solution onto a glass microscope slide for optical measurements. Linearly polarized monochromatic light (FHWM ~ 4 nm) was selected in the range 470-700 nm by means of an acousto-optic modulator coupled to a supercontinuum laser (picosecond, Fianium), and focused by an objective lens (NA = 0.42) to a diffraction limited spot. The sample was mounted inside an integrating sphere on a piezoelectric scanning stage (Laser 2000) to allow for absorption maps. The relative orientation of the polarization with respect to the individual core-shell nanowire selected for the measurement was adjusted by a half-wave plate. Both reflection and scattering were measured simultaneously by amplified silicon photodetectors (Thorlabs) coupled to lock-in amplifiers, and combined to obtain quantitative absorption.

For photoluminescence, a 532 nm continuous wave laser (WITec, 10 mW) focused through a 50X

objective was employed to excite the core-shell nanowire drop-cast from solution on a clean silicon substrate. Emission was collected through the same objective and fed to a fiber coupled spectrometer (Acton SP-2150i, Princeton Instruments) in the range of 540-1000 nm. A holographic notch filter and a long pass filter were used to block the reflection of the incoming beam.

Density functional theory (DFT) calculations

All calculations were carried out using the first-principles' Vienna Ab initio Simulation Program (VASP) [3, 4] employing density functional theory (DFT) within the Projector-Augmented Wave (PAW) method [5]. The generalized gradient approximation (GGA) formulated by Perdew, Burke, and Ernzerhof (PBE) [6] was employed for the exchange and correlation energy terms. The calculations were conducted to a level of accuracy that is sufficient for studying structural properties. The cut-off energy of the wave functions was 550.0 eV, and the cut-off energy of the augmentation functions 825.0 eV. The electronic wave functions were sampled on a $20\times20\times20$ grid for the unit cells of Ag and Cu_2O, and on a $16\times16\times2$ grid for the supercells, using the Monkhorst and Pack method. The supercells are shown in Fig. 5b,c and consist of 4 conventional cubic cells of Cu_2O and 4 conventional FCC cells of Ag (40 atoms in total). Because of the periodic boundary conditions that apply for plane-wave DFT calculations, each supercell contains two Ag/Cu_2O interfaces. The model shown in Fig. 5b shows a configuration with two equal interfaces, containing an Ag-Cu mixed layer. The model shown in Fig. 5c shows a configuration without Ag-Cu mixing, whereby the two interfaces within the supercell are not identical (one contains a layer of O atoms, the other does not). Because the stoichiometry of the two supercells is exactly the same ($Ag_{16}Cu_{16}O_8$), the energies can be directly compared. Structural optimizations were performed for the volume of the supercells and the relative positions of atoms. Different k-meshes and cut-off energies were tested to ensure a good convergence (< 2 meV/atom).

Both the volume of the simulation cells and the relative atomic positions were relaxed in order to find the lowest-energy configurations. It was found that both models were structurally stable.

The lattice mismatch and the presence of O at the interface leads to local structural relaxation. Because of the lattice mismatch between Ag and Cu_2O of 4.4%, the Ag sublattice is slightly expanded while the Cu_2O lattice is slightly compressed within the supercells. The relaxed supercells of both the mixed and unmixed models had dimensions corresponding to a lattice parameter of 4.24 Å, which is in between the DFT-calculated lattice parameters of Ag and Cu_2O of 4.15 and 4.31 Å, respectively (it is common that DFT-GGA overestimates lattice parameters in comparison to the experimental values) [7].

The interface energies, evaluated with respect to the Ag and Cu_2O bulk phases, can be calculated as follows:

$$E_{int}=\{E(Ag_{16}Cu_{16}O_8)-16\cdot E(Ag)-8\cdot E(Cu_2O)\}/2A$$

Where $E(Ag_{16}Cu_{16}O_8)$ is the total energy of the supercell, and $E(Ag)$, $E(Cu_2O)$ are the energies of the Ag and Cu_2O bulk phases. A is the area of the interface, and the factor 2 arises because there are two interfaces in the supercell. Using this formula, reasonable values for the interface energies of 0.48 Jm^{-2} and 0.51 Jm^{-2} are obtained for the mixed and unmixed models, respectively. In the experimental situation the interface energies will likely be lower because the strain at the interface will be relieved by misfit dislocations.

Absorption/scattering simulations

An FDTD (Lumerical) model was employed to simulate the 2D profile of the integrated power in the core-shell nanowire (Fig. 2d), and to simulate the nanowire array configuration (Fig. 3b). A mesh size of 0.5 nm was employed. The dielectric functions used in the model come from Palik [8].
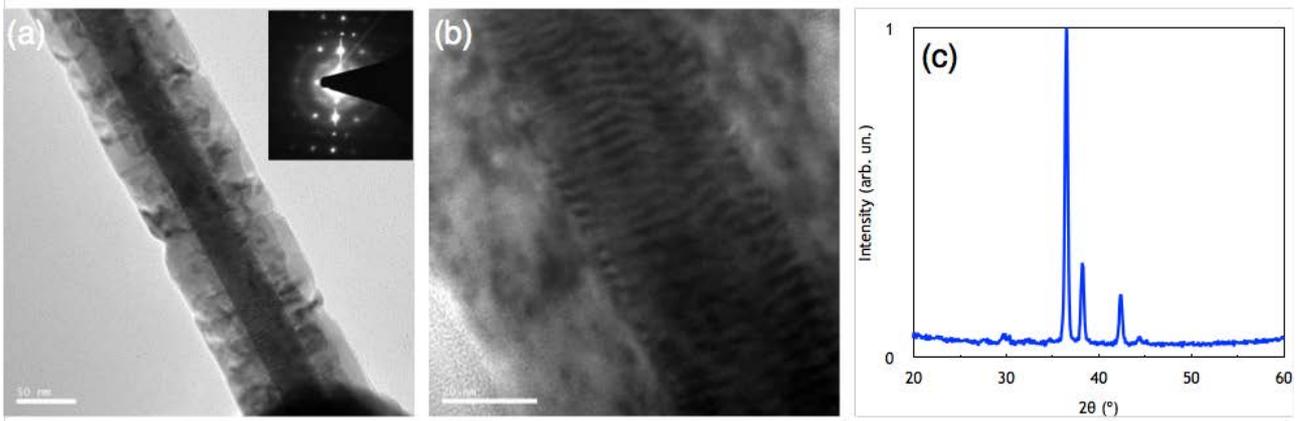
Fig. S1: (a,b) TEM image and (b) XRD of a Au-Cu$_2$O NW. Moire fringes are clearly visible in (b), indicating the crystallinity of the Cu$_2$O shell.
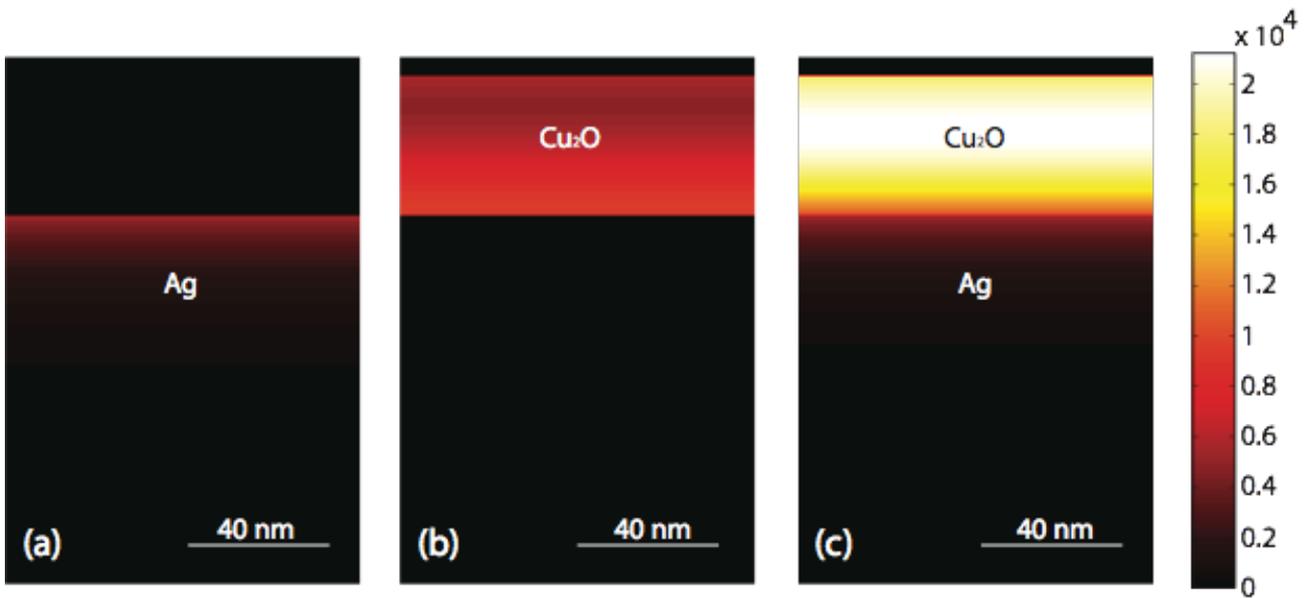
Fig. S2: Profile of the power absorbed in (a) a 100 nm Ag film, (b) a 40 nm Cu$_2$O membrane and (c) a 40nm Cu$_2$O membrane on a 100 nm Ag film. The power is weighted over the AM1.5 spectrum for photons above the band gap (290-650 nm). The color scale is in W/m^2 for a 1 V/m incident plane wave.
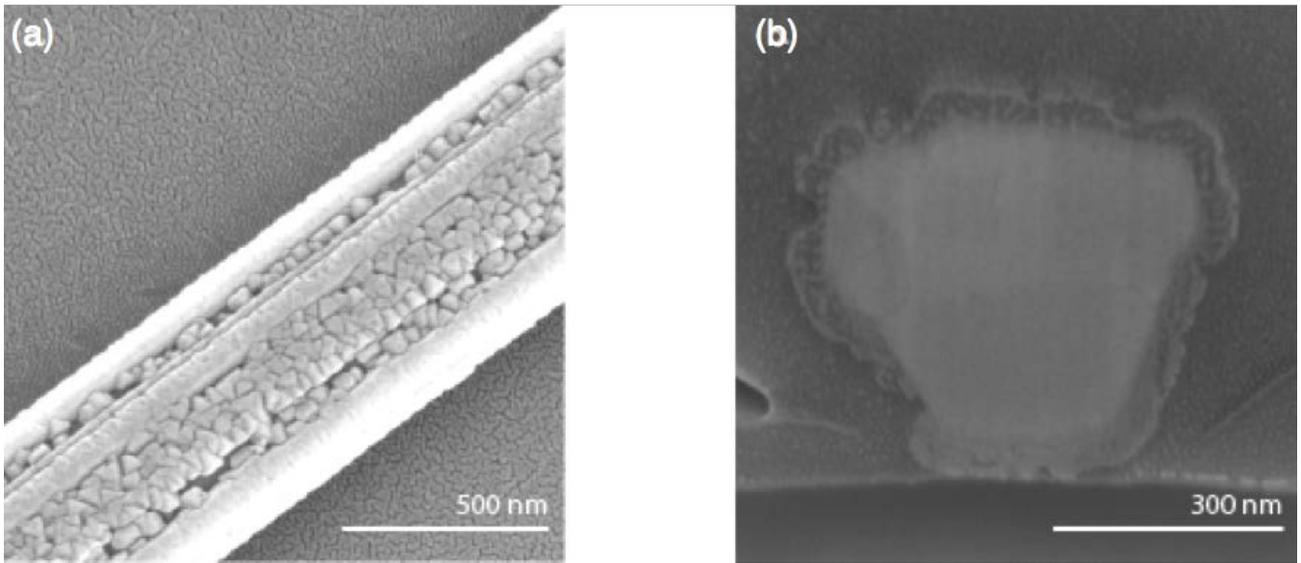
Fig. S3: (a) SE and FIB cross section of a Ag-Cu$_2$O nanowire with a thick core.
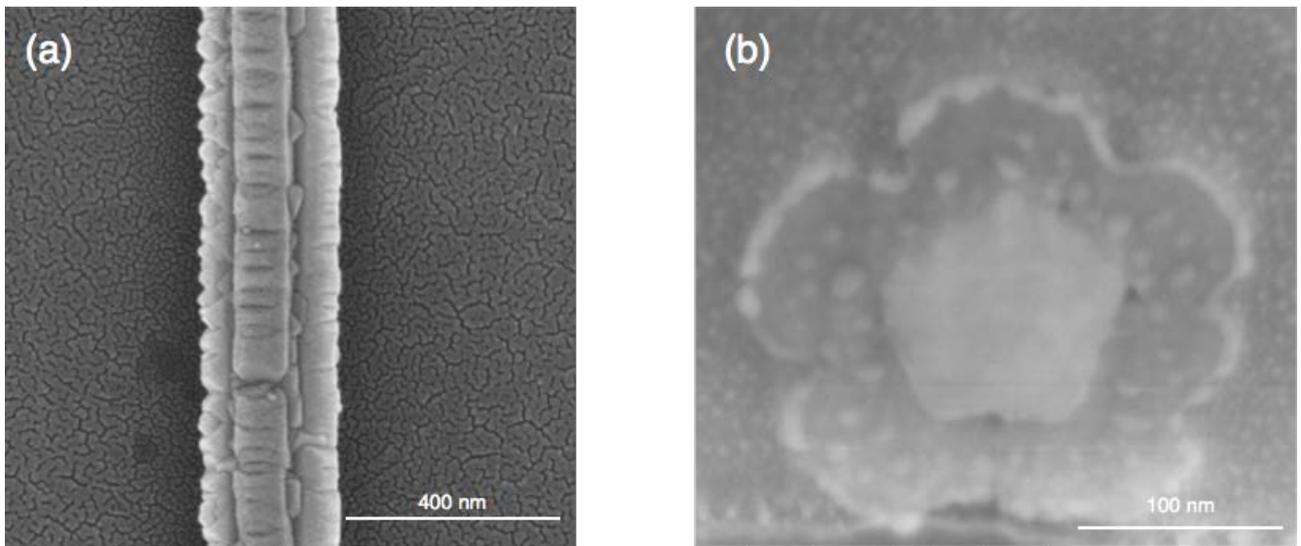
Fig. S4: SE (a) and FIB cross section (b) of the Ag-Cu$_2$O nanowire measured in Fig. 3(a).
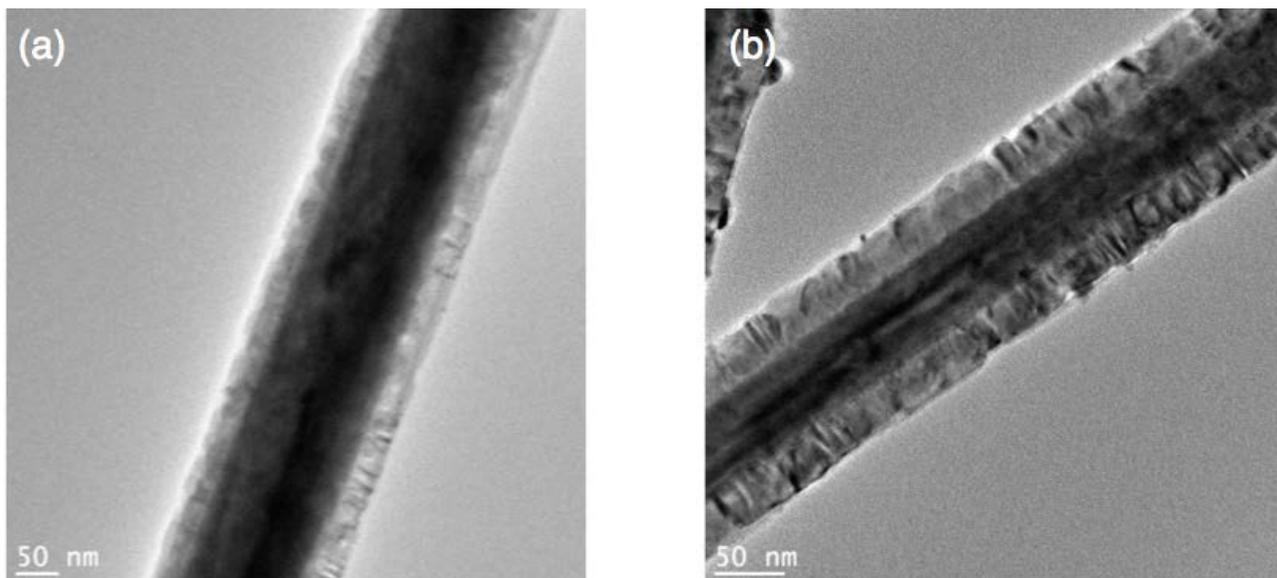
Fig. S5: (a,b) TEM images of Ag-Cu$_2$O nanowires. The images show some low-angle planar defects (b), as well as parts with a long range purely monocrystalline Cu$_2$O shell (a).
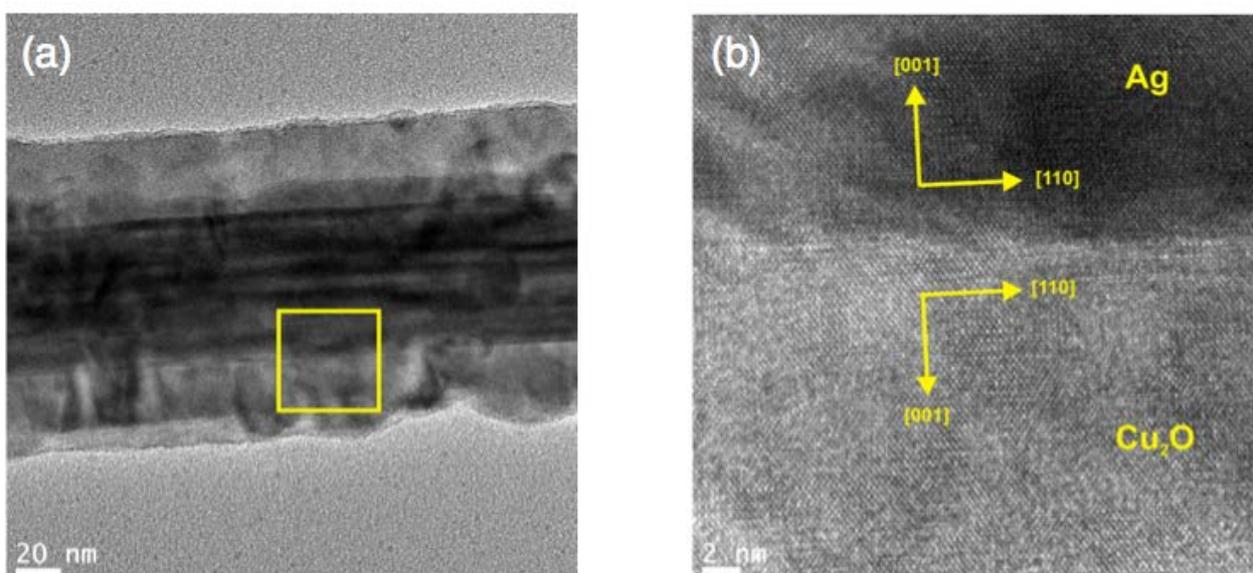
Fig. S6: (a) TEM image of Ag-Cu$_2$O nanowires. (b) HRTEM of the Ag-Cu$_2$O interface, with crystallographic directions.

References

(1) Lee, J. H.; Lee, P.; Lee, D.; Lee, S. S.; Ko, S. H. Large-Scale Synthesis and Characterization of Very Long Silver Nanowires via Successive Multistep Growth. *Crystal Growth & Design* **2012,** 12, (11), 5598-5605.

(2) Kuo, C. H.; Hua, T. E.; Huang, M. H. Au Nanocrystal-Directed Growth of Au-Cu2O Core-Shell Heterostructures with Precise Morphological Control. *Journal of the American Chemical Society* **2009,** 131, (49), 17871-17878.

(3) Kresse, G.; Hafner, J. Abinitio Molecular-Dynamics for Liquid-Metals. *Physical Review B* **1993,** 47, (1), 558-561.

(4) Kresse, G.; Furthmuller, J. Efficiency of ab-initio total energy calculations for metals and semiconductors using a plane-wave basis set. *Computational Materials Science* **1996,** 6, (1), 15-50.

(5) Kresse, G.; Joubert, D. From ultrasoft pseudopotentials to the projector augmented-wave method. *Physical Review B* **1999,** 59, (3), 1758-1775.

(6) Perdew, J. P.; Burke, K.; Ernzerhof, M. Generalized gradient approximation made simple. *Physical Review Letters* **1996,** 77, (18), 3865-3868.

(7) Perdew, J. P.; Chevary, J. A.; Vosko, S. H.; Jackson, K. A.; Pederson, M. R.; Singh, D. J.; Fiolhais, C. Atoms, Molecules, Solids, and Surfaces - Applications of the Generalized Gradient Approximation for Exchange and Correlation. *Physical Review B* **1992,** 46, (11), 6671-6687.

(8) Palik, E. D., *Handbook of Optical Constants of Solids*. New York, 1998; Vol. 1.